

## Introducing comprehensive multiphase NMR for the analysis of food: Understanding the hydrothermal treatment of starch-based foods

Andersson Barison<sup>a</sup>, Rajshree Ghosh Biswas<sup>b</sup>, Paris Ning<sup>b</sup>, Flávio Vinícius Crizóstomo Kock<sup>b,c</sup>, Ronald Soong<sup>b</sup>, Maria Carolina Bezerra Di Medeiros<sup>c,d</sup>, Andre Simpson<sup>b,\*</sup>, Luciano Morais Lião<sup>d,\*</sup>

<sup>a</sup> NMR Centre, Department of Chemistry, Federal University of Paraná, Curitiba, Paraná, Brazil

<sup>b</sup> Environmental NMR Centre, Department of Physical and Environmental Sciences, University of Toronto, Scarborough, Ontario, Canada

<sup>c</sup> Nuclear Magnetic Resonance Laboratory, Federal University of São Carlos, São Carlos, São Paulo, Brazil

<sup>d</sup> Nuclear Magnetic Resonance Laboratory, Institute of Chemistry, Federal University of Goiás, Goiânia, Goiás, Brazil

### ARTICLE INFO

#### Keywords:

Hydrothermal treatment  
Starch-based foods  
Structural changes  
Comprehensive multiphase NMR

### ABSTRACT

Cooking is essential for preparing starch-based food, however thermal treatment promotes the complexation of biopolymers, impacting their final properties. Comprehensive Multiphase (CMP) NMR allows all phases (liquids, gels, and solids) to be differentiated and monitored within intact samples. This study acts as a proof-of-principle to introduce CMP-NMR to food research and demonstrate its application to monitor the various phases in spaghetti, black turtle beans, and white long-grain rice, and how they change during the cooking process. When uncooked, only a small fraction of lipids and structurally bound water show any molecular mobility. Once cooked, little “crystalline solid” material is left, and all components exhibit increased molecular dynamics. Upon cooking, the solid-like components in spaghetti contains signals consistent with cellulose that were buried beneath the starches in the uncooked product. Thus, CMP-NMR holds potential for the study of food and related processes involving phase changes such as growth, manufacturing, and composting.

### 1. Introduction

The starch gelatinization process, in which starch is subjected to hydrothermal treatment, as in cooking, is the main functional property studied for this type of matrix. The rheological characteristics acquired by gelatinized starch stem mainly from the disruption of the molecular ordering of the granules, their swelling, a fusion of the crystalline structures, loss of birefringence, change in viscosity, and solubilization (Sukhija et al., 2016).

Starch granules consist of two main polysaccharide categories, namely amylose and amylopectin, both composed of  $\alpha$ -(1  $\rightarrow$  4) linked D-glucopyranosyl moieties. While amylose is essentially a linear structure, amylopectin is highly branched, interconnected through  $\alpha$ -(1  $\rightarrow$  6) glycosidic linkages (Pascoal et al., 2013). Both biopolymers are arranged into a complex semi-crystalline granular structural conformation, resulting from aggregates of double helices. The ratio of crystalline to amorphous material in the starch granule varies from 10 % to 50 %, depending on the botanical origin of the starch and composition

(amylose/amylopectin ratio and amylopectin branch length) (Kovrljica et al., 2020). Amylose may be present in free or lipid complexed forms. The linear nature of amylose chains confers its physicochemical properties and distinct rheological behavior from the amylopectin crystal moiety. Amylose chains can form films and complexes with alcohols, lipids, and acids (Silva et al., 2019). On the other hand, amylopectin is structurally and functionally more important than amylose, mainly due to its high capacity for water absorption during the cooking process. It is mainly responsible for granule swelling and changes in the visco-amylographic properties.

The thermal process during cooking promotes the complexation of biopolymers, impacting the final properties of the food. The interaction of carbohydrate molecules with lipids is known to impact food characteristics, depending on the chemical composition (Morrison et al., 1984). The presence of fatty acids in food can impact viscosity and solubility of carbohydrates. In addition, rheological properties of starch-based cooked foods are influenced by the type of fatty acids present and their ability to complex (Kaur & Singh, 2000). In this context,

\* Corresponding authors.

E-mail addresses: [andre.simpson@utoronto.ca](mailto:andre.simpson@utoronto.ca) (A. Simpson), [lucianoliao@ufg.br](mailto:lucianoliao@ufg.br) (L.M. Lião).

<https://doi.org/10.1016/j.foodchem.2022.133800>

Received 29 January 2022; Received in revised form 27 June 2022; Accepted 25 July 2022

Available online 26 July 2022

0308-8146/© 2022 Elsevier Ltd. This article is made available under the Elsevier license (<http://www.elsevier.com/open-access/userlicense/1.0/>).

understanding the nature of interactions and the behavior of the components that make up the food matrices is fundamental for developing optimal preparation, processing of foods, as well as, understanding nutritional potential.

Nuclear magnetic resonance (NMR) spectroscopy is a powerful molecular-level technique that allows the investigation of complex chemical structures and their interactions. NMR has long been used to study food-related products, and the first application of HR-MAS NMR to food samples was likely that of the analysis of durum wheat flours from different geographical areas of southern Italy (Sacco et al., 1998). Nowadays,  $^1\text{H}$  HR-MAS has been established as one of the most common NMR spectroscopy techniques in food science (Jensen & Bertram, 2019; Santos et al., 2015).

Regarding changes in the chemical composition during the hydrothermal treatment, NMR has been used to probe water status within cereals and its related products as well as to trace water movement (hydration and diffusion) and distribution (Kovrljija & Rondeau-Mouro, 2017). Structural changes in solid networks have been observed before using solid-state NMR (Foster, et al., 1996; Nowacka-Perrin et al., 2022). During the cooking process, the food structure changes dramatically as starch granules start to gelatinize. NMR has been used to study the gelatinization and thermal processes occurring during cooking as well as retrogradation (Kovrljija & Rondeau-Mouro, 2017). In these works, while samples were analyzed in their natural state, NMR can only provide information on select phases (solution and gel-like). For example, in the pioneering work from Sacco et al. (Sacco et al., 1998), a commercial HR-MAS probe was used which provided information on the solution and gel-like phases but was unable to access the solid phase of wheat.

Traditional solution-state NMR probes use lower-power electronics along with a lock channel, pulsed-field gradient which provides excellent line shapes, although only for dissolved or liquid samples. The HR-MAS probes use the magic angle for spinning and for gradient, aligned along the spin axis, as well as corresponding susceptibility stators, which allowed the study of gel-like or swollen materials in their natural state, such as vegetables and tissue intact animals. However, HR-MAS probes are designed with low power circuitry and cannot handle the high-power RF fields required for cross-polarization or high-power decoupling, which is essential for most solid-state NMR experiments (Smernik et al., 2004). On the other hand, solid-state NMR or CP-MAS probes were designed to handle high-power RF fields. However, they are dedicated to studying rigid solid samples, thus do not have the hardware to investigate components in the solution and gel-like phases (Courtier-Murias et al., 2012). Magnetic Resonance Imaging (MRI) has been, thus far, often used to study the cooking process. Nevertheless, as it can only drive low-power RF fields, only mobile components such as water and oil can be detected (Stapley et al., 1997). With this in mind, technology to date, have been unable to study all phases (solution, gel, and solids) simultaneously, limiting insights into molecular flux between and across phases. Thus, the only option was to potentially use separate probes, although this only holds for the most superficial structural studies and most importantly is very limited regarding investigations targeting kinetic transfer between the phases or changes from one phase into another.

Considering this, comprehensive multiphase (CMP) NMR was introduced in 2012 and incorporates all of the aforementioned aspects, including magic angle spinning, magic angle gradient, lock, full susceptibility matching, and high-power RF handling. In summary, CMP-NMR refers to the use of a single NMR probe that allows all components, in all phases, as well as interfaces, compartmentalization, and binding to be investigated *in situ* in unaltered samples (Fortier-McGill et al., 2017). In addition, CMP-NMR makes it possible to monitor the molecular flux between different phases during the cooking process in a non-destructive holistic manner (Courtier-Murias et al., 2012).

CMP-NMR is becoming a useful tool in a range of scientific fields (Santos et al., 2016), but application of CMP-NMR to food chemistry is still in its infancy with only loosely related agricultural studies of seed

structure (Fortier-McGill et al., 2017), germination (Santos et al., 2016), and early growth (Lam et al., 2014) reported to date. The goal of this work is to introduce CMP-NMR to investigate starch-based food and the hydrothermal treatment focusing on structural information that can be extracted from  $^1\text{H}$  and  $^{13}\text{C}$  CMP-NMR spectra at natural abundance. Specifically, spaghetti pasta, black turtle beans, and white long-grain rice were selected for the study as they represent basic foods of global importance.

## 2. Material and methods

### 2.1. Samples and hydrothermal treatment

All the starch-based samples used in this work, including untreated long-grain white rice, dry spaghetti pasta (wheat semolina), black turtle beans, and edible oil (for comparison purposes), were purchased from local supermarkets in Toronto, ON, Canada. The samples were cooked in boiling water (no salt) and the cooking times varied as reported below. The samples were added after the water started boiling to simulate cooking pasta in a traditional kitchen. All samples were cooked as is, except for the beans, which were presoaked to soften them, along with the removal of the seed coats (and any embryos) to decrease the cooking time. The food was cooked for the following times: Spaghetti pasta – 3, 6, and 15 (full cooked) min; Rice – 5, 10, and 20 (full cooked) min; Black beans –10 and 30 (full cooked) min.

### 2.2. Sample preparation

NMR measurements were performed on the uncooked food, as well as, at different cooking time intervals. However, as it was impossible to insert the entirety of the uncooked samples directly into 4-mm MAS rotors due to their size, rice and bean samples were minimally crushed and the chunks were placed into the rotor. In the case of black beans, the seed coats and embryos were removed prior to being placed in the rotor to mimic cooked beans as closely as possible. The food was then transferred into full volume (i.e., without any upper or lower spacers) 4-mm MAS rotors and sealed with standard Kel-F caps, resulting in a  $\sim 105\ \mu\text{L}$  probe volume. Whereas for pasta, two 1.7 mm diameter spaghetti sticks were cut at the same size as the rotor length and shaved with the aid of a razor blade leaving  $\sim 70\ \mu\text{L}$  unoccupied by the spaghetti sticks. After cooking, the supernatant water was removed, and the softened samples were cut into small pieces and directly inserted into 4-mm MAS rotors, as mentioned above. The exception being for the cooked food and edible oil, the rotors were sealed with a small upper Kel-F spacer/Kel-F sealing screw to prevent the leakage of fluids during spinning. With the Kel-F cap and inserts in place, the rotor had an active volume of  $\sim 75\ \mu\text{L}$ .

### 2.3. NMR Spectroscopy

#### 2.3.1. Standard 1D NMR

All NMR experiments were acquired on a Bruker AVANCE III NMR spectrometer operating at 11.7 Tesla, fitted with a prototype 4-mm four radiofrequency channels ( $^2\text{H}$ ,  $^1\text{H}$ ,  $^{13}\text{C}$ , and  $^{31}\text{P}$ ) CMP-MAS probe with a magic angle gradient (Courtier-Murias et al., 2012). Samples were spun at 6666 Hz since this spinning speed results in a rotor period of 150  $\mu\text{s}$ , allowing simple rotor synchronization of pulses and delays. All experiments were performed at room temperature without lock (i.e., no  $\text{D}_2\text{O}$  was added to the samples, and the lock system was turned off during acquisition). This is somewhat unusual for CMP-NMR studies, which are usually run locked, but performed here as the  $\text{H}_2\text{O}$  signals (which rapidly exchange and disappear in presence of  $\text{D}_2\text{O}$ ) were of particular interest.

All  $^1\text{H}$  spectra were acquired with 16 k time-domain points distributed on a spectral width of 15 ppm, providing a digital resolution of 0.91 Hz, 2 s recycle delay, and 256 scans. When required, water suppression was performed using pre-saturation ( $\sim 50\ \text{Hz}$  RF field).

$^{13}\text{C}\{^1\text{H}\}$  NMR (except solid-state experiments) was performed with 16 k time-domain points distributed over a 248 ppm spectral width, providing a digital resolution of 3.81 Hz. A 2 s recycle delay, 10 k scans and *waltz16* low-power inverse gated decoupling were used as well.

$^{13}\text{C}$  solid-state cross-polarization magic angle spinning (CP-MAS) were acquired with TOSS-243 (Song et al., 1993) sideband suppression, rotor synchronization and a ramp of 80–100 % during the 1 ms contact time, 2 k time-domain points distributed over a 400 ppm spectral width, providing a digital resolution of 48.8 Hz, 2 s recycle delay and 10,206 (multiples of the 243 phase cycle) scans and *spinal-64* for high power  $^1\text{H}$  decoupling were used.

Spectra were processed by applying an exponential Lorentzian multiplication with a line broadening factor of 1.0, 3.0, and 25.0 Hz to the FIDs for  $^1\text{H}$ ,  $^{13}\text{C}$ , and CP-MAS experiments, respectively, followed by Fourier transformation using a zero-filling factor of 2. Phase and baseline corrections were manually performed.

### 2.3.2. Spectral editing

Diffusion based spectral editing (DE) of both  $^1\text{H}$  and  $^{13}\text{C}$  were been performed with a bipolar pulse pair longitudinal encode/decode (BPPLIED) sequence (Wu et al., 1995), using encoding/decoding gradient pulses of 1.8 ms at  $\sim 50$  Gauss/cm and a diffusion time of 180 ms.

For CP-MAS NMR based editing, a  $T_2$  filter was achieved by adding a CPMG building block on the  $^1\text{H}$  channel prior to cross polarization. The relaxation filter consisted of 1 or 2 echoes separated by a time ( $\tau$ ) of 7.5  $\mu\text{s}$  prior to cross-polarization (total 15  $\mu\text{s}$  and 30  $\mu\text{s}$  respectively) to remove signals from rigid/crystalline domains (Courtier-Murias et al., 2012).

Individual phases (liquids, gels, semi-solids, and rigid solids) were recovered by weighted subtractions from appropriate controls. These approaches are described in detail in previous work (Courtier-Murias et al., 2012) and an editing example is shown in Fig. S1. The freely diffusing species S1b (termed inverse diffusion editing) are recovered by subtracting the diffusion edited spectrum (S1c) (components with restricted diffusion) from a diffusion control (restricted and free components) (S1f). The diffusion control is the BPPLIED sequence with all delays set but the main encoding/decoding gradients turned off. The “gel-like or restricted diffusion” phase is provided by the diffusion editing itself (S1c).

A special approach termed Relaxation Recovery Arising from Diffusion Editing (RADE) is also applied. Here the components that would otherwise relax during the diffusion delay and could otherwise be missed are recovered. These components are the fastest relaxing “proton-detectable” materials and tend to be generally classed as semi-solids, i.e., they have enough mobility to appear in  $^1\text{H}$  NMR, but account for the fastest relaxing component. The RADE sub-spectrum (S1d) is created by the difference between a diffusion sequence where both delays and gradient are set to zero (i.e., detects all components) and the diffusion reference (Fig. S1f) experiment (where the delays are set but the diffusion gradient remains turned off). The only disparity between the 2 datasets is the relaxation of components that are being lost during the diffusion delays which are recovered by difference in the RADE spectrum (S1d). For the weighted subtractions, the spectra were scaled until the dominant component being subtracted was nulled, leaving a difference sub-spectrum containing positive signals (Courtier-Murias et al., 2012).

The  $^1\text{H}$  pulse width was calibrated for each sample, considering the slowest  $^1\text{H}$  relaxation. On the other hand, adamantane was used to calibrate the  $^{13}\text{C}$  pulses.  $^1\text{H}$  and  $^{13}\text{C}$  NMR chemical shifts were referenced against the signal from the terminal methyl group of saturated/high degree saturation fatty acid moieties at 0.83 and 14.1 ppm, respectively (Sacco et al., 1998).

## 3. Results and discussion

Single pulse NMR (i.e., without spectral editing) provides an overview of all the components with enough dynamics to be easily detected using  $^1\text{H}$  NMR. Generally, this tends to be soluble and swollen species as rigid solids exhibit strong  $^1\text{H}$ – $^1\text{H}$  dipole interactions that can lead to linewidths of 10's or 100's of KHz wide. The  $^1\text{H}$  NMR spectra acquired with low-power decoupling for the uncooked foods (i.e., long-grain white rice, spaghetti pasta, and black turtle beans) in their dried-state as purchased, were dominated by structural water, and triacylglycerols (TAG), see Fig. 1. While the materials are predominately starch containing, carbohydrates were not observed in the  $^1\text{H}$  NMR (Fig. 1) indicating all carbohydrates in the dried form are present as rigid solids. The black turtle beans were found to have the highest amount of TAG lipids, while white rice presented a lower TAG content, as expected. It is important to note that this study uses commercial white rice which contains only the starchy endosperm (white rice) and does not include the germ (rice kernel), where TAG lipids are often found in higher amounts (Khattoon & Gopalakrishna, 2004).

### 3.1. $^1\text{H}$ based spectral editing

Spectral editing can further emphasize components from specific phases in the food samples. Diffusion editing (DE) emphasizes the NMR signals from components that have restricted or slow diffusion coefficients. Here components with restricted diffusion are defined as compounds that remain in the same physical position throughout the diffusion delay (i.e., move less than  $\sim 1$   $\mu\text{m}$  in 180 ms). Those signals are refocused at the end of the diffusion period while components that move within the sample are not. Species that survive diffusion editing include small compounds bound to surfaces and very large macromolecules that hardly exhibit any translational diffusion. Here the TAG species survive the diffusion editing in the uncooked samples (see Fig. 2B for an example with spaghetti). Here the TAG signal (0.8–2.9 and 5.2–5.4 ppm) after diffusion editing is intense and the difference (Fig. 2C) i.e., dissolved molecules [Inverse Diffusion Edited (IDE) spectrum] show practically no signals indicating that the TAG are trapped within the spaghetti's solid phase starch matrix and are not free to move positions. Similar results have been described by Fortier-McGill et al. 2017 and Lam et al. 2014

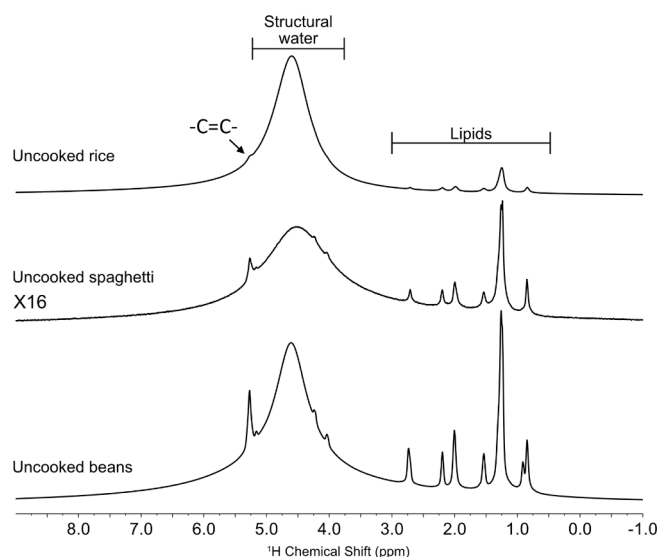


**Fig. 1.** Standard 1D  $^1\text{H}$  NMR acquired with low-power decoupling, showing that with the exception of water, TAG lipids dominate the “dynamic” components observed in uncooked starch-based food. Carbohydrates signals (that resonate predominately between 3 and 4 ppm) were not seen. All spectra acquired under MAS (6666 KHz) at 11.7 Tesla.

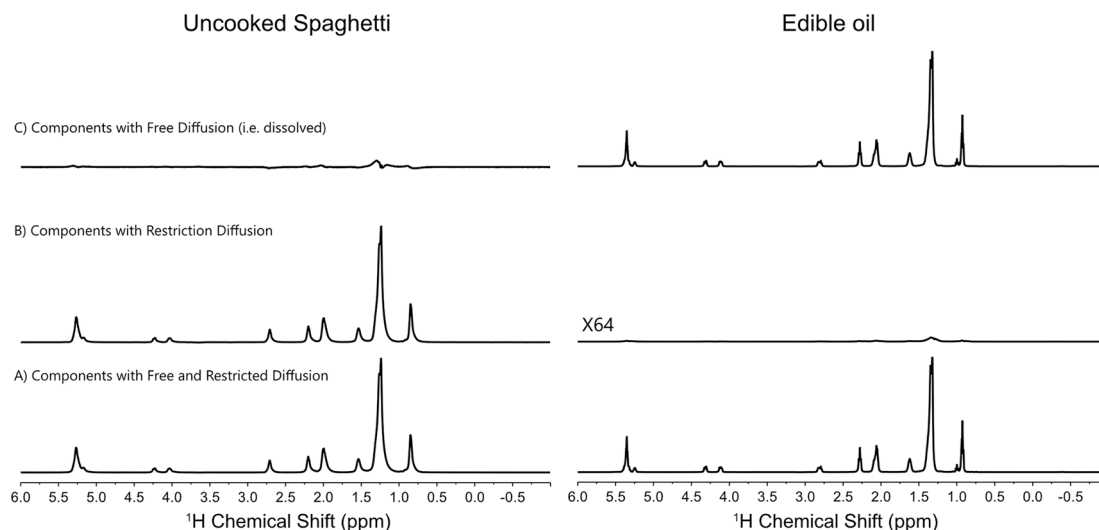


**Fig. 2.**  $^1\text{H}$  NMR spectra (with low-power decoupling) highlighting diffusion edited (DE) experiments for spaghetti and a neat edible oil. A) is the diffusion control where the delays for diffusion are set but the diffusion gradient is set to zero. Here all components with free and restricted diffusion are observed. B) represents the Diffusion Editing (DE) experiment, which retains only components that have restricted diffusion (both diffusion delays and gradient turned on). C) represents the freely diffusing molecules by difference [inverse diffusion edited (IDE, spectrum A - spectrum B)]. The experiments show that TAG components exhibit minimal diffusion when trapped inside the starch-based spaghetti. All spectra acquired under MAS (6666 KHz) at 11.7 Tesla.

while monitoring structural changes within broccoli, corn, and wheat seeds by means of CMP-NMR (Fortier-McGill et al., 2017; Lam et al., 2014). As such TAG stored in droplets/micelles would have restricted diffusion consistent with the results observed. Also the formation of starch-lipid (i.e., fatty acids) complexes have been identified in previous NMR studies (Zabar et al., 2009) which could also partially explain lipids with restricted diffusion.

To demonstrate the concept further, a liquid edible oil sample was included in the experimental design for comparison. In this case, DE experiments suppress >99 % of the oil signals consistent with a sample exhibiting free diffusion. The small remaining signal in the diffusion editing spectrum could be self-associations of a small fraction within the edible oil. Indeed, the inverse diffusion edited spectra [IDE, after subtraction (2A-B)] showed that in the case of the neat edible oil, the majority of TAG components are free to diffuse as expected. In summary, when considered together, Fig. 2 clearly shows that CMP-NMR can differentiate between bound and free TAG, and in the case of dry spaghetti, all the TAG molecules are bound within the starch matrix and are not free to diffuse.

Additionally, the relaxation recovery arising from diffusion editing (RADE) NMR experiment can provide complementary information on the faster relaxing  $^1\text{H}$  detectable components in the sample, most analogous to “semi-solids” or “rigid-gels”. When applied to the dried spaghetti (Fig. S2) the RADE spectrum show some contributions from TAG, which could be consistent with a more rigid fraction possibly from cell wall components, micelles, or vesicles within the spaghetti. Interestingly there is a strong contribution from the broad water signal in RADE. This water exhibits fast relaxation (hence it dominated the RADE spectrum) and a broad lineshape consistent with entrapped and/or hydrogen bonded “structural water” within the dry spaghetti. Potentially this trapped water could be very interesting, seeing as agricultural products such as wheat and food are often thoroughly dried for longer shelf life and long-term storage. Thus, the ability of CMP-NMR to easily detect the structural water component could be useful in determining the efficiency of drying and could potentially be linked to the shelf life of a product (Mathlouthi, 2001).

### 3.2. Carbon detected NMR

Carbon detected NMR experiments are complementary to  $^1\text{H}$  based

approaches. Here the  $^{13}\text{C}\{^1\text{H}\}$  experiments shown in Fig. 3 are performed with low-power decoupling, thus the hydrogen nuclei from components in the rigid solids, which have linewidths far greater than the decoupling field, will be strongly attenuated. As such, the carbon spectra in Fig. 3, are somewhat analogous to the  $^1\text{H}$  spectra shown in Fig. 1, in that components with molecular mobility and dynamics will be emphasized while rigid solids will be suppressed. Fig. 3 shows the  $^{13}\text{C}\{^1\text{H}\}$  spectra for all uncooked samples which contain only signals from TAG lipid components, consistent with these components being present in more dynamic environments (such as gel-like and semi-solid) rather than as rigid solids. Given that similar amounts of uncooked food were packed in each rotor, the amount of dynamic TAG content in each sample can be ranked as beans > spaghetti > rice based on SNR. In contrast, other components, including carbohydrates, were not visible, indicating that in the uncooked foods, the carbohydrates exhibit little molecular dynamics and are present as crystallites and amorphous structure which make up rigid solids, thus not detectable when  $^{13}\text{C}\{^1\text{H}\}$  NMR experiments using low-power  $^1\text{H}$  decoupling are employed.

CP-MAS NMR experiments can be used to detect crystalline and amorphous solids (rigid components) efficiently. The intensity of signals in CP-MAS depends on the strength and the number of dipolar interactions between carbon and its surrounding hydrogen nuclei. In solutions and dynamic species, these dipoles are modulated by molecular motion which makes CP-MAS extremely inefficient (Courtier-Murias et al., 2012). However, for solids with rigid bonds, cross-polarization is efficient and CP-MAS editing is applied in this study to emphasize the rigid components present in the food matrices. Signals in solid-state spectra tend to be broader than their more dynamic counterparts in gel-like/semi-solid and liquid states, and consequently, solid-state NMR spectra are often less resolved. Although, by combining CP-MAS with other CMP-NMR approaches (e.g., DE, RADE, and IDE), cross-assignments are possible, which in turn helps to identify components in both phases.

Fig. 4A shows the CP-MAS spectra for the uncooked food matrices. It was observed that the aliphatic signals (10–50 and 170–180 ppm) from TAG are very low in the beans and hardly detectable in the spaghetti and rice. This is consistent with the TAG/lipids components in uncooked starch-based foods being found predominately in the more dynamic environments thus contributing less to the solid-phase. The solid-state component is dominated by carbohydrates signals (50–110 ppm)

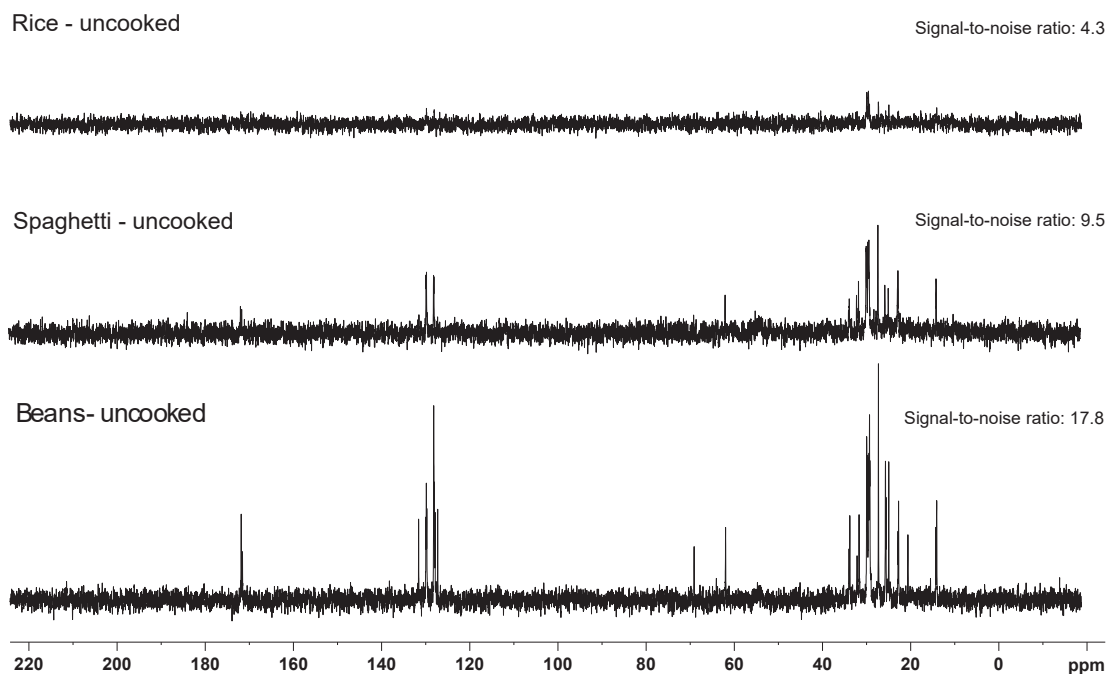


Fig. 3.  $^{13}\text{C} \{^1\text{H}\}$  spectra acquired with low-power decoupling, showing that TAG lipids were the only components with enough molecular dynamics (i.e., gel-like, and semi-solid phases) to be detected using low power  $^1\text{H}$  decoupling in the dry uncooked samples. All spectra acquired under MAS (6666 KHz) at 11.7 Tesla.

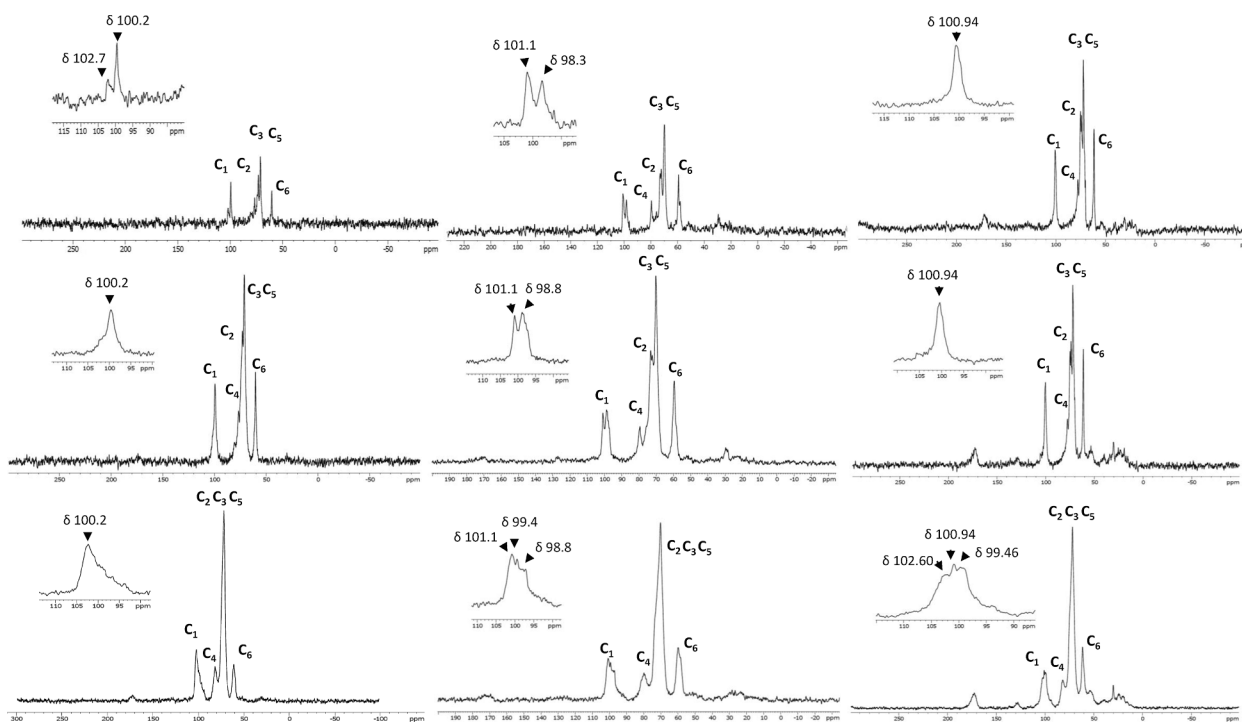


Fig. 4. (A)  $^{13}\text{C}$  CP-MAS spectra for rice, spaghetti, and beans, uncooked, highlighting all components: rigid + dynamic solids. (B)  $^{13}\text{C}$  CP-MAS spectra for rice, spaghetti, and beans, intermediary cooked, highlighting all components: rigid + dynamic solids. (C)  $^{13}\text{C}$  CP-MAS spectra for rice, spaghetti, and beans, full cooked, highlighting all components: rigid + dynamic solids. All spectra acquired under MAS (6666 KHz) at 11.7 Tesla.

consistent with starch.

The hydrothermal treatment applied to the rice, spaghetti, and beans promoted a change in the structural organization of the crystalline unit cells of the starch granules. We can observe in Fig. 4A (uncooked) a triple C-1 peak from anomeric carbon for starch of the bean and spaghetti's wheat, too, typical of double helices of amylopectin when packeted into a mostly monoclinic arrangement. While, B-type

polymorph was observed for spaghetti cooked at both times (Fig. 4B and 4C), characterized by the double signal for anomeric peak and the emergence of the C-type arrangement and more mobile amorphous chains, as already observed for complex wheat foods (Sivam et al., 2013). Bean starch after cooking showed structural reorganization with total loss of A pattern and transition to C-type, characteristic of complexation processes with polyphenols, proteins, and lipids. The

spectral pattern of rice, on the other hand, reveals a type V starch characteristic of granules essentially composed of amylose. For this same starch, an extra peak for C-1 can be seen at 102.7 ppm, suggesting a chemical complexation involving the amylose chains (Hu et al., 2013).

The amorphous/dynamic solids can be differentiated from the rigid solids through the use of a very short CPMG filter prior to cross-polarization (Courtier-Murias et al., 2012). The filter allows the fast relaxing components (Claridge, 2016) (i.e., crystalline solids) to relax, leaving only the pool of protons from the dynamic solids to undergo subsequent cross-polarization. This experiment termed  $T_2$  filtered CP-MAS (CP- $T_2$ ) is shown in Fig. S3 and again is dominated mainly by starch resonances. The rigid crystalline solids can be recovered via difference, by subtracting S3A (all solids) and S3B (dynamics solids). Again, the rigid solids show very similar signals from starch. Starch, in its native form, is a semi-crystalline structure containing both amorphous ( $C_4$  signal at 78–86 ppm range) and crystalline regions. According to the literature (Lopez-Rubio et al., 2008; Zobel, 1988), cereals such as wheat and rice have significant contributions from both forms. Here the relative signal between the rigid (crystalline) and dynamic (amorphous) domains is  $\sim 50:50$  in the uncooked foods, suggesting that the solid detecting capabilities of CMP-NMR could be useful to isolate and study the different solid sub-phases in food if required. It is essential mainly because it is possible to analyze the components of rigid structures and their structural changes, dispensing with the drying or freeze-drying steps, which significantly impact the structural organization since water effectively contributes to the structuring of the granules (Tan et al., 2007).

### 3.3. Changes during hydrothermal treatment

Arguably, the most exciting potential for CMP-NMR is following changes during a process, which in this study arises from alterations during cooking.

Fig. 5 highlights the changes seen in the  $^1\text{H}$  NMR detected spectral editing experiments upon cooking. As discussed in Fig. 1A, structural water is trapped within the solid matrix before cooking and manifests as a broad, wide resonance center around  $\sim 4.7$  ppm (Fig. 5A). After cooking, the food matrix swells, and the trapped/structural water

becomes dynamic and sharp. The narrowing of the water signal reflects the gelatinization of the starch during cooking, clearly observed by CMP-NMR. This is consistent with the water in the dried food being in a bound rigid form, likely structural water associated with macromolecules such as starch and protein (Micklander et al., 2008; Mortensen et al., 2005). When spectral editing is applied, it can be seen that starch components (3.2–3.4 and  $\sim 5.35$  ppm) dominate the swollen components (i.e., those with restricted diffusion (Fig. 5BII)). Conversely, the spectral profile for the dissolved components (Fig. 5BIII) contains only a few signals corresponding to the food swelling but staying as a swollen mass rather than dissolving into the surrounding water, as is the case with cooked rice. Similar results are seen for the other food studied here, which are summarized in Fig. S10. Although relative to the spaghetti and beans, more of the rice starch is seen to dissolve. This is consistent with the fact that rice “milk” [a beverage made from rice (Koyama & Kitamura, 2014) can be made after extensive cooking of the rice. In each case, after cooking, the material swells and the starch predominately take on a dynamic gel-like nature, with little signal seen in the dissolved phase (with the exception of rice). Note that starch swelling is the main process observed here, related to the hydrothermal treatment of cooking in excess water. However, investigations regarding water mobility and starch transformations in other systems, such as breads, cakes, or deep frying, grilling, and reductions, could also be studied since CMP-NMR can be used to follow chemical and physical changes.

The RADE experiment is also helpful to follow the cooking process via  $^1\text{H}$  NMR. Here the semi-solids are emphasized (see Fig. S11) but rigid solids are suppressed. In the uncooked foods, the starch is too “solid-like” to be detected by RADE, but as the cooking process progresses the starch swells and becomes a semi-solid. The RADE data in this case supports the diffusion edited data, where the RADE biases the semi-solids while diffusion editing biases the more dynamic swollen gels with longer relaxation times.

Finally, it is worth noting that while considerably less sensitive, carbon NMR provides a quite clear and easy to interpret overview of the hydrothermal treatment. Fig. 6A shows the dynamic components, which in the solids show only TAG signals. However, after 6 mins of cooking, starch now clearly contributes to the dynamic phase. After 15 mins of cooking (fully cooked) the contribution of starch in the dynamic fraction

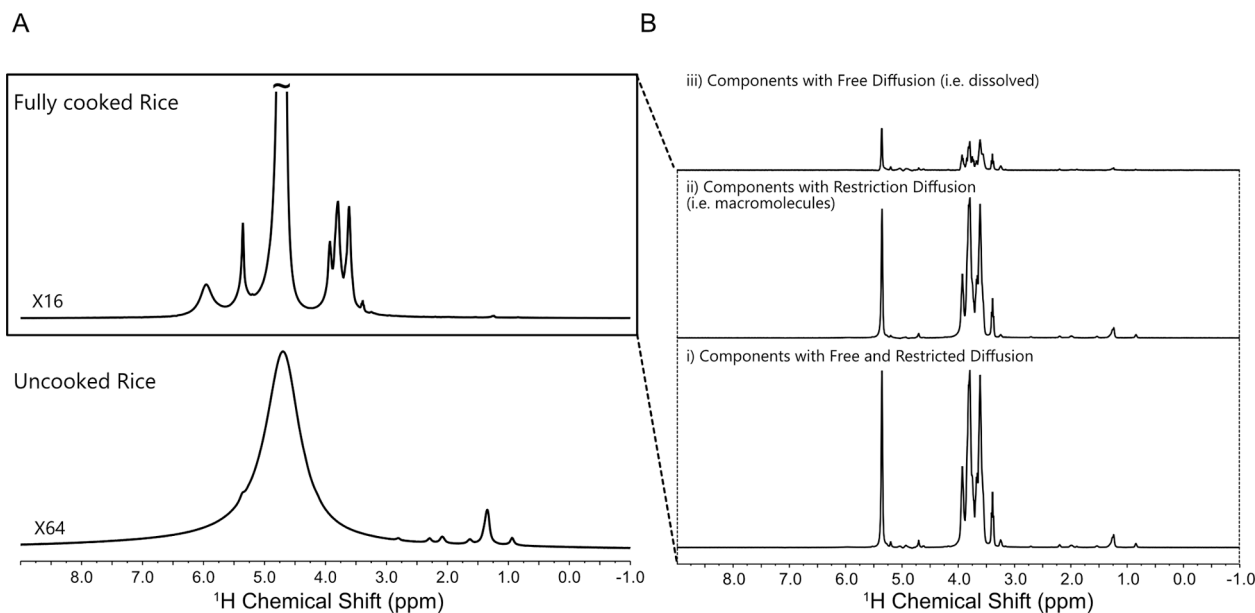
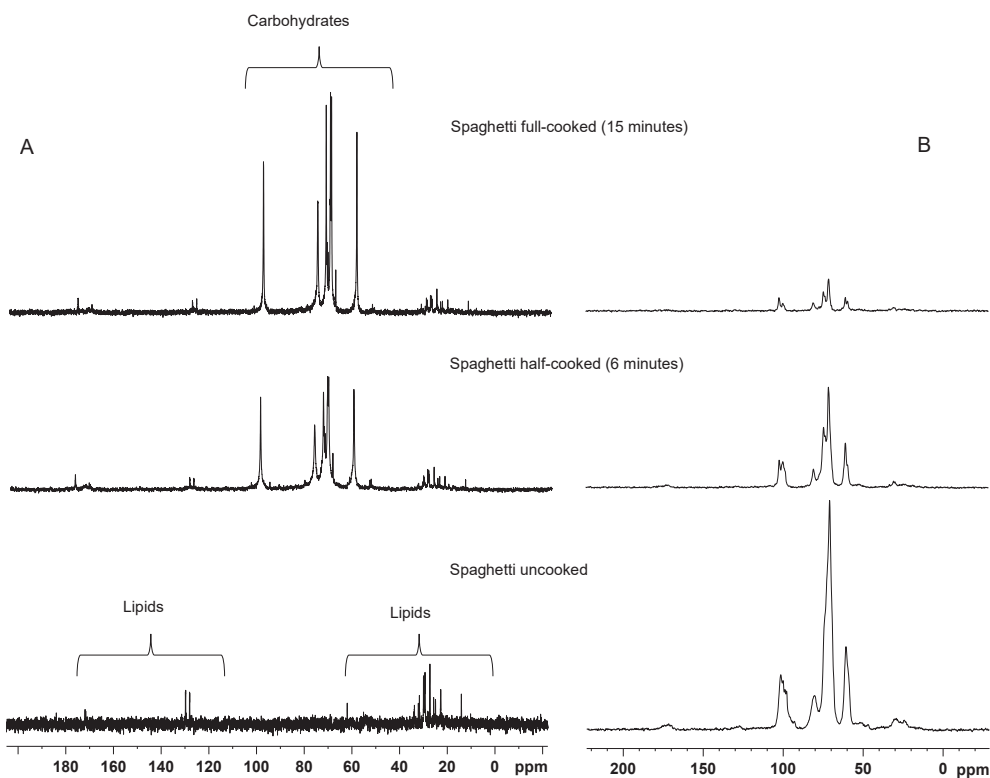


Fig. 5. (A)  $^1\text{H}$  NMR reference spectra obtained with low-power decoupling for uncooked and fully cooked rice, highlighting the sharp signal from non-structural water (i.e., freely diffusing water) after hydrothermal treatment. No water suppression pulse sequence was applied. (B) Diffusion based editing NMR spectra showing that there are few dissolved components, and the swollen food behaves like a swollen “gel” dominated by starch. Water suppression was applied in B. All spectra acquired under MAS (6666 KHz) at 11.7 Tesla.



**Fig. 6.** (A) Standard  $^{13}\text{C}$  NMR with low-power decoupling of uncooked (bottom), half-cooked (6 min, middle), and full-cooked (15 min, top) spaghetti. (B)  $^{13}\text{C}\{^1\text{H}\}$  CP-MAS NMR spectra of the same sample. The data shows that as a function of cooking time, the starches disappear from the solid-phase (CP-MAS), and as they swell, appear in the standard carbon experiment corresponding to gelatinization. All spectra acquired under MAS (6666 KHz) at 11.7 Tesla.

increases further. As expected, the opposite trend is seen in the CP-MAS NMR which monitors the solid fraction. In the dry spaghetti the signal is strong due to efficient dipoles in the solid starch. However, after 6 mins of cooking the signal has dropped by about 60 %, which after 15 mins of cooking drops by about 90 %. This indicates only a small fraction (10 % of less) of the spaghetti retains a solid-like character after cooking.

Considering, that cooking pasta “Al Dente” is important in upscale restaurants and mass-produced higher end precooked Italian food, it is possible to conceive that one day NMR could have a role in monitoring the cooking process and quality control for batch consistency. The carbon approach is appealing as it does not suffer from water contributions, and the phases can be monitored without complicated editing experiments (note only Fig. 6 simply uses standard ZGIG (low power inverse gated  $^1\text{H}$  decoupling) and CP experiments (Hughes et al., 2014).

The  $^1\text{H}$  and  $^{13}\text{C}\{^1\text{H}\}$  NMR spectra and spectral editing for all starch food matrices addressed in this work can be observed in the supporting information (Figs. S2–S12). Results are consistent with those seen for spaghetti and show the start of gelatinization upon cooking. The results could be very important for understanding the time different foods require to become fully cooked. For example, in Figs. S4 and S5 it is clear significant changes continue between 6 and 20 min (spaghetti) and 5 to 20 mins (rice). Conversely, hardly any spectral features change for beans between 10 and 30 mins, indicating they are likely close to complete hydration after only 10 mins. Figures S7–S9 confirm these observations through carbon (rather than proton) NMR. In Fig. S12, the assigned  $^1\text{H}$  NMR spectrum of fully cooked spaghetti. Assignments were completed based on Nowacka-Perrin et al., 2022.

#### 4. Conclusions

Much effort has been put in to monitoring and understanding the gelatinization process by employing analytical techniques, including viscometry, optical microscopy, electron microscopy, differential

scanning calorimetry (DSC), X-ray diffraction, nuclear magnetic resonance (NMR) spectroscopy, and Fourier transform infrared (FTIR) spectroscopy.

Most recently, simultaneous X-ray scattering could check the structural transformation by studying the process via the difference in the macroscopic property during starch gelatinization. However, structural characterization at the atomic level, such as monitoring the specific hydrogens in the macromolecular structure, intra-granular water, and extra granular water, can be achieved through NMR spectroscopy, representing a great power of understanding concerning water mobility and starch transformation. Here it is shown that CMP-NMR spectroscopy has considerable potential for understanding food and food-related processes such as cooking. It is highly complementary to approaches such as time-domain NMR as it correlates physical changes to the components responsible for the changes via spectroscopy (Mathlouthi, 2001; Kovrljija & Rondeau-Mouro, 2017).

In this proof-of-principle study, only starch-based foods were studied and only 1D NMR was explored. As such, carbohydrates dominated the spectral profiles and observed changes were largely restricted to starch swelling. However, in foods such as fruits, vegetables, and meats, that have a greater diversity of structural entities including nutrients, amino acids, tannins, etc. 2D NMR could be extremely useful. For example, the greater spectral dispersion and connectivity information from 2D NMR could be used to track how nutrients are released from the solid-state (i. e., dried food) and how they degrade/transform during hydrothermal treatment. A similar CMP-NMR approach was very informative in understanding the metabolic processes behind seed germination and growth (Fortier-McGill et al., 2017) and the same holds for studying processes within food. If required, approaches to quantify the amount of carbon in each phase have been published (Ning et al., 2020) and while somewhat laborious, are available if estimates of the quantitative distribution of carbon in each phase are required.

Future studies are of course not restricted only to the cooking process

and could be expanded to understand molecular changes in food as it ages (including correlating phase changes to metabolites of spoilage), during growth, impact of additives (preservatives, fertilizer), impact of processing (both food preparation and manufacturing), as-well as gelling, flocculation, drying, and dissolution processes – all central to food stability and preservation. More advanced NMR studies could also be employed, for example specific experiments to study  $^{12}\text{C}$ – $^{13}\text{C}$  bond formation have been introduced (Jenne et al., 2019), which could provide unique information as to the fate of additives, be it carbon sources for plant growth or preservatives in food. The experiment could explain exactly, at the bond level, how the carbon is utilized and parallel experiments for studying non-covalent interactions of probe molecules have also been introduced (Lane et al., 2019). Using a very recent technique termed DREAMTIME, it should also be possible to monitor user defined suites of molecules (Jenne et al., 2022) during food-related processes. Such approaches could be extremely advantageous for monitoring biomarkers of food spoilage which are directly linked to food poisoning (Cheng et al., 2015) and could provide a better understanding of food longevity and preservation from a molecular perspective. If required, such approach could permit monitoring of targets down to the ppb level.

With relation to recent hardware developments, the use of  $^{13}\text{C}$  optimized CMP-NMR probes (Ning, Lane, Biswas, et al., 2021) could provide >100 % more carbon sensitivity, extremely useful for studying foods where water suppression could be challenging or where the additional spectral dispersion afforded by the wider chemical shift range of  $^{13}\text{C}$  is required for assignment or monitoring. Similarly, larger diameter probes could be useful, by simply either 1) shortening studies through the use of larger amounts of biomass, or 2) allowing the analysis of larger intact entities such as berries and seeds (Ning, Lane, Ghosh Biswas, et al., 2021).

In summary, the current study acts as a simple proof-of-principle study to introduce CMP-NMR for food research. CMP-NMR is the only modern analytical technique that can provide detailed molecular information on all components (solids, gels, and liquids) in unaltered samples and thus hold considerable potential for the future of food analysis.

## Funding

This work was supported by Natural Sciences and Engineering Research Council (NSERC) (Alliance (ALLRP 549399) and Discovery Programs (RGPIN-2019-04165)) and Brazilian foundation agencies (CAPES 88881.170844/2018-0, L.M.L.), (CAPES/FAPPR 99999.000640/2016-06, A.B.), (FAPESP 2018/16040-5 and 2019/14770-9 for F.V.C.K., and 2019/16135-9 for M.C.B.D.M).

## Author contributions

AB, AS and LML conceptualization and designed the experiments; AB, RGB, PN and MCBDM performed the experiments; AB, FVCK, RS and LML analysed the data; RS, AS and LML supervised the experiments; AB, RGB, FVCK and MCBDM organized and wrote the manuscript; FVCK, AS and LML reviewed and edited the manuscript; AB and LML: resources; AS funding acquisition.

## Ethical approval

This article does not contain any studies with human participants or animals performed by any of the authors.

## Declaration of Competing Interest

The authors declare that they have no known competing financial interests or personal relationships that could have appeared to influence the work reported in this paper.

## Data availability

No data was used for the research described in the article.

## Appendix A. Supplementary data

Supplementary data to this article can be found online at <https://doi.org/10.1016/j.foodchem.2022.133800>.

## References

- Cheng, J., Gao, R., Li, H., Wu, S., Fang, J., Ma, K., ... Dong, F. (2015). Evaluating potential markers of spoilage foods using a metabolic profiling approach. *Food Analytical Methods*, 8(5), 1141–1149. <https://doi.org/10.1007/S12161-014-9999-Z/FIGURES/6>
- Claridge, T. D. W. (2016). High-Resolution NMR Techniques in Organic Chemistry: Third Edition. In *High-Resolution NMR Techniques in Organic Chemistry: Third Edition*. Elsevier Ltd. 10.1016/C2015-0-04654-8.
- Courtier-Murias, D., Farooq, H., Masoom, H., Botana, A., Soong, R., Longstaffe, J. G., ... Simpson, A. J. (2012). Comprehensive multiphase NMR spectroscopy: Basic experimental approaches to differentiate phases in heterogeneous samples. *Journal of Magnetic Resonance*, 217, 61–76. <https://doi.org/10.1016/j.jmr.2012.02.009>
- Fortier-McGill, B. E., Dutta Majumdar, R., Lam, L., Soong, R., Liaghati-Mobarhan, Y., Sutrisno, A., ... Simpson, A. J. (2017). Comprehensive multiphase (CMP) NMR monitoring of the structural changes and molecular flux within a growing seed. *Journal of Agricultural and Food Chemistry*, 65(32), 6779–6788. <https://doi.org/10.1021/acs.jafc.7b02421>
- Foster, T. J., Ablett, S., McCann, M. C., & Gidley, M. J. (1996). Mobility-resolved  $^{13}\text{C}$ -NMR spectroscopy of primary plant cell walls - Foster - 1996 - Biopolymers - Wiley Online Library. *Biopolymers*, 39(1), 51–66.
- Hu, X., Wei, B., Zhang, B., Li, H., Xu, X., Jin, Z., & Tian, Y. (2013). Interaction between amylose and 1-butanol during 1-butanol-hydrochloric acid hydrolysis of normal rice starch. *International Journal of Biological Macromolecules*, 61, 329–332. <https://doi.org/10.1016/j.ijbiomac.2013.07.020>
- Hughes, C. E., Williams, P. A., & Harris, K. D. M. (2014). “CLASSIC NMR”: An in-situ NMR strategy for mapping the time-evolution of crystallization processes by combined liquid-state and solid-state measurements. *Angewandte Chemie International Edition*, 53(34), 8939–8943. <https://doi.org/10.1002/anie.201404266>
- Jenne, A., Bermel, W., Michal, C. A., Gruschke, O., Soong, R., Ghosh Biswas, R., ... Simpson, A. J. (2022). DREAMTIME NMR spectroscopy: Targeted multi-compound selection with improved detection limits. *Angewandte Chemie International Edition*. <https://doi.org/10.1002/anie.202110044>
- Jenne, A., Soong, R., Bermel, W., Sharma, N., Masi, A., Tabatabaei Anaraki, M., & Simpson, A. (2019). Focusing on “the important” through targeted NMR experiments: An example of selective  $^{13}\text{C}$ – $^{12}\text{C}$  bond detection in complex mixtures. *Faraday Discussions*, 218, 372–394. <https://doi.org/10.1039/C8FD00213D>
- Jensen, H. M., & Bertram, H. C. (2019). The magic angle view to food: Magic-angle spinning (MAS) NMR spectroscopy in food science. *Metabolomics*, 15(3), 1–25. <https://doi.org/10.1007/S11306-019-1504-7>
- Kaur, K., & Singh, N. (2000). Amylose-lipid complex formation during cooking of rice flour. *Food Chemistry*, 71(4), 511–517. [https://doi.org/10.1016/S0308-8146\(00\)00202-8](https://doi.org/10.1016/S0308-8146(00)00202-8)
- Khatoun, S., & Gopalakrishna, A. G. (2004). Fat-soluble nutraceuticals and fatty acid composition of selected Indian rice varieties. *Journal of the American Oil Chemists' Society*, 81(10), 939–943. <https://doi.org/10.1007/s11746-004-1005-5>
- Kovrljija, R., Goubin, E., & Rondeau-Mouro, C. (2020). TD-NMR studies of starches from different botanical origins: Hydrothermal and storage effects. *Food Chemistry*, 308, Article 125675. <https://doi.org/10.1016/J.FOODCHEM.2019.125675>
- Kovrljija, R., & Rondeau-Mouro, C. (2017). Multi-scale NMR and MRI approaches to characterize starchy products. *Food Chemistry*, 236, 2–14. <https://doi.org/10.1016/J.FOODCHEM.2017.03.056>
- Koyama, M., & Kitamura, Y. (2014). Development of a new rice beverage by improving the physical stability of rice slurry. *Journal of Food Engineering*, 131, 89–95. <https://doi.org/10.1016/J.JFOODENG.2014.01.030>
- Lam, L., Soong, R., Sutrisno, A., de Visser, R., Simpson, M. J., Wheeler, H. L., ... Simpson, A. J. (2014). Comprehensive multiphase NMR spectroscopy of intact  $^{13}\text{C}$ -labeled seeds. *Journal of Agricultural and Food Chemistry*, 62(1), 107–115. <https://doi.org/10.1021/jf4045638>
- Lane, D., Liaghati Mobarhan, Y., Soong, R., Ning, P., Bermel, W., Tabatabaei Anaraki, M., ... Simpson, A. J. (2019). Understanding the fate of environmental chemicals inside living organisms: NMR-based  $^{13}\text{C}$  isotopic suppression selects only the molecule of interest within  $^{13}\text{C}$ -enriched organisms. *Analytical Chemistry*, 91(23), 15000–15008. <https://doi.org/10.1021/acs.analchem.9b03596>
- Lopez-Rubio, A., Flanagan, B. M., Gilbert, E. P., & Gidley, M. J. (2008). A novel approach for calculating starch crystallinity and its correlation with double helix content: A combined XRD and NMR study. *Biopolymers*, 89(9), 761–768. <https://doi.org/10.1002/bip.21005>
- Mathlouthi, M. (2001). Water content, water activity, water structure and the stability of foodstuffs. *Food Control*, 12(7), 409–417. [https://doi.org/10.1016/S0956-7135\(01\)00032-9](https://doi.org/10.1016/S0956-7135(01)00032-9)
- Micklander, E., Thybo, A. K., & van den Berg, F. (2008). Changes occurring in potatoes during cooking and reheating as affected by salting and cool or frozen storage – A LF-

- NMR study. *LWT – Food Science and Technology*, 41(9), 1710–1719. <https://doi.org/10.1016/J.LWT.2007.10.015>
- Morrison, W. R., Milligan, T. P., & Azudin, M. N. (1984). A relationship between the amylose and lipid contents of starches from diploid cereals. *Journal of Cereal Science*, 2(4), 257–271. [https://doi.org/10.1016/S0733-5210\(84\)80014-4](https://doi.org/10.1016/S0733-5210(84)80014-4)
- Mortensen, M., Thybo, A. K., Bertram, H. C., Andersen, H. J., & Engelsen, S. B. (2005). Cooking effects on water distribution in potatoes using nuclear magnetic resonance relaxation. *Journal of Agricultural and Food Chemistry*, 53(15), 5976–5981. <https://doi.org/10.1021/JF0479214>
- Ning, P., Lane, D., Biswas, R. G., Soong, R., Schmidig, D., Frei, T., ... Simpson, A. J. (2021). Comprehensive multiphase NMR probehead with reduced radiofrequency heating improves the analysis of living organisms and heat-sensitive samples. *Analytical Chemistry*, 93(29), 10326–10333. <https://doi.org/10.1021/ACS.ANALCHEM.1C01932>
- Ning, P., Lane, D., Ghosh Biswas, R., Jenne, A., Bastawrous, M., Soong, R., ... Simpson, A. J. (2021). Expanding current applications and permitting the analysis of larger intact samples by means of a 7 mm CMP–NMR probe. *Analyst*, 146(14), 4461–4472. <https://doi.org/10.1039/D1AN00809A>
- Ning, P., Lane, D., Soong, R., Schmidig, D., Frei, T., De Castro, P., ... Simpson, A. J. (2020). Comprehensive multiphase NMR—A powerful tool to understand and monitor molecular processes during biofuel production. *ACS Sustainable Chemistry & Engineering*, 8(47), 17551–17564. <https://doi.org/10.1021/acssuschemeng.0c07205>
- Nowacka-Perrin, A., Steglich, T., Topgaard, D., & Bernin, D. (2022). In situ 13C solid-state polarization transfer NMR to follow starch transformations in food. *Magnetic Resonance in Chemistry*, 1–7. <https://doi.org/10.1002/MRC.5253>
- Pascoal, A. M., Di-Medeiros, M. C. B., Batista, K. A., Leles, M. I. G., Lião, L. M., & Fernandes, K. F. (2013). Extraction and chemical characterization of starch from *S. lycocarpum* fruits. *Carbohydrate Polymers*, 98(2), 1304–1310. <https://doi.org/10.1016/J.CARBPOL.2013.08.009>
- Sacco, A., Neri Bolsi, I., Massini, R., Spraul, M., Humpfer, E., & Ghelli, S. (1998). Preliminary investigation on the characterization of durum wheat flours coming from some areas of South Italy by means of 1 H high-resolution magic angle spinning nuclear magnetic resonance. *Journal of Agricultural and Food Chemistry*, 46(10), 4242–4249. <https://doi.org/10.1021/jf971113d>
- Santos, A. D. C., Blumkin, L., Masoom, H., Soong, R., Barison, A., & Simpson, A. J. (2016). Spectral background from commercially available D2O: An important consideration for trace analysis using cryoprobes. *Magnetic Resonance in Chemistry*, 54(5), 377–381. <https://doi.org/10.1002/mrc.4410>
- Santos, A. D. C., Fonseca, F. A., Lião, L. M., Alcantara, G. B., & Barison, A. (2015). High-resolution magic angle spinning nuclear magnetic resonance in foodstuff analysis. *TrAC Trends in Analytical Chemistry*, 73, 10–18. <https://doi.org/10.1016/J.TRAC.2015.05.003>
- Silva, E. M. S., Peres, A. E. C., Silva, A. C., Leal, M. C. D. M., Lião, L. M., & De Almeida, V. O. (2019). Sorghum starch as depressant in mineral flotation: Part 1 – Extraction and characterization. *Journal of Materials Research and Technology*, 8(1), 396–402. <https://doi.org/10.1016/J.JMRT.2018.04.001>
- Sivam, A. S., Waterhouse, G. I. N., Zujovic, Z. D., Perera, C. O., & Sun-Waterhouse, D. (2013). Structure and dynamics of wheat starch in breads fortified with polyphenols and pectin: An ESEM and solid-state CP/MAS 13C NMR spectroscopic study. *Food and Bioprocess Technology*, 6(1), 110–123. <https://doi.org/10.1007/s11947-011-0699-z>
- Smernik, R. J., Oliver, I. W., & McLaughlin, M. J. (2004). Changes in the nature of sewage sludge organic matter during a twenty-one-month incubation. *Journal of Environmental Quality*, 33(5), 1924–1929. <https://doi.org/10.2134/jeq2004.1924>
- Song, Z., Antzutkin, O. N., Feng, X., & Levitt, M. H. (1993). Sideband suppression in magic-angle-spinning NMR by a sequence of 5  $\pi$  pulses. *Solid State Nuclear Magnetic Resonance*, 2(3), 143–146. [https://doi.org/10.1016/0926-2040\(93\)90032-1](https://doi.org/10.1016/0926-2040(93)90032-1)
- Stapley, A. G. F., Hyde, T. M., Gladden, L. F., & Fryer, P. J. (1997). NMR imaging of the wheat grain cooking process. *International Journal of Food Science & Technology*, 32(5), 355–375. <https://doi.org/10.1046/J.1365-2621.1997.00122.X>
- Sukhija, S., Singh, S., & Riar, C. S. (2016). Physicochemical, crystalline, morphological, pasting and thermal properties of modified lotus rhizome (*Nelumbo nucifera*) starch. *Food Hydrocolloids*, 60, 50–58. <https://doi.org/10.1016/j.foodhyd.2016.03.013>
- Tan, I., Flanagan, B. M., Halley, P. J., Whittaker, A. K., & Gidley, M. J. (2007). A method for estimating the nature and relative proportions of amorphous, single, and double-helical components in starch granules by 13 C CP/MAS NMR. *Biomacromolecules*, 8(3), 885–891.
- Wu, D. H. D. H., Chen, A., & Johnson, C. S. C. S. (1995). An improved diffusion-ordered spectroscopy experiment incorporating bipolar-gradient pulses. *Journal of Magnetic Resonance, Series A*, 115(2), 260–264. <https://doi.org/10.1006/jmra.1995.1176>
- Zabar, S., Lesmes, U., Katz, I., Shimoni, E., & Bianco-Peled, H. (2009). Studying different dimensions of amylose-long chain fatty acid complexes: Molecular, nano and micro level characteristics. *Food Hydrocolloids*, 23(7), 1918–1925. <https://doi.org/10.1016/J.FOODHYD.2009.02.004>
- Zobel, H. F. (1988). Molecules to granules: A comprehensive starch review. *Starch – Stärke*, 40(2), 44–50. <https://doi.org/10.1002/STAR.19880400203>